

ORIGINAL ARTICLE

Langerhans cells and SFRP2/Wnt/beta-catenin signalling control adaptation of skin epidermis to mechanical stretching

Joanna K. Ledwon¹  | Elbert E. Vaca¹ | Chiang C. Huang² | Lauren J. Kelsey¹ | Jennifer L. McGrath¹ | Jacek Topczewski³ | Arun K. Gosain¹ | Jolanta M. Topczewska^{1,3}

¹Department of Surgery, Plastic Surgery Division, Northwestern University Feinberg School of Medicine, Stanley Manne Children's Research Institute, Ann and Robert H. Lurie Children's Hospital of Chicago, Chicago, Illinois, USA

²University of Wisconsin, Joseph J Zilber School of Public Health, Milwaukee, Illinois, USA

³Department of Pediatrics, Northwestern University Feinberg School of Medicine, Stanley Manne Children's Research Institute, Ann and Robert H. Lurie Children's Hospital of Chicago, Chicago, Illinois, USA

Correspondence

Arun K. Gosain and Joanna K. Ledwon, Department of Plastic and Reconstructive Surgery, 225 East Chicago Avenue, Chicago, IL, 60611, USA.

Emails: argosain@luriechildrens.org (A.K.G.); jledwon@luriechildrens.org (J.K.L.)

Funding information

This work was supported by a NIBIB grant 1R21EB021590-01A1 awarded to Arun K. Gosain (PI), by a NIBIB grant (NIBIB) 1R01AR074525-01A1 to Adrian B. Tepole (PI), and by Ann and Robert H Lurie Children's Hospital Faculty Practice Plan

Abstract

Skin can be mechanically stimulated to grow through a clinical procedure called tissue expansion (TE). Using a porcine TE model, we determined that expansion promptly activates transcription of *SFRP2* in skin and we revealed that in the epidermis, this protein is secreted by Langerhans cells (LCs). Similar to well-known mechanosensitive genes, the increase in *SFRP2* expression was proportional to the magnitude of tension, showing a spike at the apex of the expanded skin. This implies that *SFRP2* might be a newly discovered effector of mechanotransduction pathways. In addition, we found that acute stretching induces accumulation of b-catenin in the nuclei of basal keratinocytes (KCs) and LCs, indicating Wnt signalling activation, followed by cell proliferation. Moreover, TE-activated LCs proliferate and migrate into the suprabasal layer of skin, suggesting that LCs rebuild their steady network within the growing epidermis. We demonstrated that in vitro hrSFRP2 treatment on KCs inhibits Wnt/b-catenin signalling and stimulates KC differentiation. In parallel, we observed an accumulation of KRT10 in vivo in the expanded skin, pointing to TE-induced, SFRP2-augmented KC maturation. Overall, our results reveal that a network of LCs delivers SFRP2 across the epidermis to fine-tune Wnt/b-catenin signalling to restore epidermal homeostasis disrupted by TE.

KEYWORDS

epidermis, Langerhans cells, mechanical forces, mechanotransduction, SFRP2, skin growth, tissue expansion, Wnt signalling

1 | INTRODUCTION

Tissue expansion (TE) is a clinical procedure that stimulates skin growth through repetitive mechanical stretching.^{1,2} Despite a long history of clinical application, the molecular mechanisms involved in skin response to TE are still largely unknown. Porcine skin is used extensively in biomedical research to study wound healing, infectious

disease and radiation, because it closely resembles the human homologue.³ Given this, porcine became an excellent animal model to study the mechanical properties and molecular mechanisms of TE.⁴⁻⁸ Our previous study on genome-wide transcriptional changes in TE revealed that mechanical forces from the expander activate pathways related to immune response, metabolism, muscle contraction and cytoskeleton organization in a time-dependent manner.⁴ We

This is an open access article under the terms of the Creative Commons Attribution License, which permits use, distribution and reproduction in any medium, provided the original work is properly cited.

© 2022 The Authors. *Journal of Cellular and Molecular Medicine* published by Foundation for Cellular and Molecular Medicine and John Wiley & Sons Ltd.

noted *SFRP2* (Secreted frizzled-related protein 2), a well-known modulator of Wnt signalling, among the most upregulated genes during expansion.⁴ Here, we continue our investigation into the role of *SFRP2* in skin growth and regeneration stimulated by TE.

SFRP2 is a potent signalling molecule recognized for its ability to modulate Wnt/beta-catenin signalling. It belongs to a family of proteins that can bind directly to Wnt ligands to prevent receptor binding and activation of Wnt signalling.⁹ *SFRP2* has multiple biological roles in diverse cellular processes, including tissue development¹⁰ and tissue homeostasis.¹¹ It has previously been reported that *SFRP2* is involved in proliferation and energy metabolism in cardiac fibroblasts¹¹ and regulates cell proliferation, survival and a superior regenerative phenotype of mesenchymal stem cells.^{12,13} In hyperpigmented skin, such as melasma, solar lentigo and acutely UV-irradiated skin, increased expression of *SFRP2* resulted in enhanced melanogenesis through positive regulation of Wnt/beta-catenin signalling.¹⁴ An agonistic function of *SFRP2* was also shown as its synergy with Wnt16b increased cancer cell proliferation, migration and drug resistance.¹⁵ Together, the literature indicates that *SFRP2* modulates Wnt signalling and contributes to skin development and homeostasis, but it has not previously been implicated in skin mechanotransduction.

Langerhans cells (LCs), dendritic cells of the epidermis, are involved in maintaining epidermal health and tolerance to commensal microorganisms, and in adaptive immune response to pathogens invading the epidermis.^{16,17} LCs originate from embryonic precursors, mainly liver monocytes, and are recruited to the epidermis during development. Of note, LCs are also capable of local self-renewal, as shown in wound healing, inflammation and homeostatic conditions.^{18,19} LC characteristics are very similar between different species, including human, porcine and mouse²⁰ and CD207/Langerin is a popular marker, also used in this study, to identify epidermal LCs.²¹

Here, we describe *SFRP2* as a new target gene of mechanotransduction which modulates Wnt/beta-catenin signalling and the behaviour of keratinocytes (KCs). We show that secretion of *SFRP2* by LCs plays a key role in maintaining epidermal homeostasis. While a typical TE procedure takes several weeks before reconstructive surgery, we learned that stretching activates regenerative mechanisms within hours.

2 | MATERIALS AND METHODS

2.1 | Porcine tissue expansion models

Animals used in this study were treated as approved by protocol from Northwestern University Institutional Animal Care and Use Committee (IACUC# LCH14-006), and NIH standards provided in the 'Guide for the Care and Use of Laboratory Animals'. We have performed eight protocols of tissue expansion (TE) using hairless 5–6 weeks old females Yucatan minipigs,²² which were selected due to a minimal skin pigmentation. The rectangular tissue expanders (PMT Corp.), commonly used in the clinical settings, were placed anteriorly over the ribs (TE models: Ex-1h, Ex-3d, Ex-10d^{(7+3)*},

Ex-10d⁽⁷⁺³⁾) or posteriorly over the abdomen (TE models: Ex-24h, Ex-7d, Ex-14d^{(7+7)*}, Ex-14d⁽⁷⁺⁷⁾) (Figure S1a,b). The '*' indicates the models with a double 30 ml injection. The expanders were inflated once with 60 ml of saline for 1 hour, 24 hours, 3 days or 7 days prior to euthanasia, or twice of either 30 ml or 60 ml at 10 and 3 days or 14 and 7 days prior to euthanasia, per approved protocol. The three skin biopsies for RNA study and one for histological evaluation were collected in each category: the apex ('a'), the middle ('b') and the periphery ('d') of the expanded skin immediately prior to euthanasia (Figure S1c). The biopsies from the similar locations on the contralateral sites were used as controls.

2.2 | RNA isolation

The full-thickness skin punch biopsies were preserved in All Protect Tissue Reagent (Qiagen) according to manufacturer's recommendations, and RNA was extracted as described previously.⁴ Briefly, tissue was homogenized using the 3 mm zirconium beads (Benchmark Scientific) and BeadBug homogenizer. Total RNA was isolated using RNeasy Mini Kit (Qiagen) followed by DNase I digestion. The quality and quantity of RNA were evaluated by NanoDrop (Thermo Fisher), the agarose gel electrophoresis and fluorometric method (Qubit™).

2.3 | Real-time PCR analysis

Synthesis of cDNA was performed using the High-capacity cDNA Reverse Transcription kit (Life Technologies) and 200 ng of total RNA according to the manufacturer's recommendations. The Real-time PCR analysis (qRT-PCR) was performed on StepOnePlus Real-Time PCR system (Applied Biosystems) using TaqMan Assay (Applied Biosystems) in a 10 µl reaction mixture per manufacturer recommendations. Cycling conditions included an initial denaturation at 95°C for 15 min, then 45 cycles at 95°C for 15 s and 60°C for 1 min. The cycle quantification values were calculated using the threshold cycle method. Fold change of gene expression was calculated with the $2^{-\Delta\Delta C_T}$ method.²³ For the animal studies, the gene expression results were normalized to *B2M* expression and for in vitro experiments with human cells results were normalized to the normalization factor, which was calculated as a geometric mean of three reference genes: *GAPDH*, *HPRT* and *HMBS1*.

2.4 | Histology

The tissue biopsies were fixed in 10% neutral buffer formalin for 24 hours at room temperature. The post-fixation processing, performed with Spin Tissue Processor (Thermo Fisher), included 1 hour fixation in 10% neutral buffer formalin, 30 min incubation in Pen-Fix (Richard-Allan Scientific), dehydration in ethanol series (1 × 80%, 2 × 95%, 2 × 100%) 30 min each, then incubation in two changes of xylene for 1 hour each, and in three changes of paraffin for 60 min

each. Samples were embedded using paraffin embedding centre and cut at 5 μm using Microtome (EC350-2, Thermo Fisher). The sections were mounted on Superfrost Plus Microscope Slides (Thermo Fisher) using Eco-Mount medium (Biocare Medical) and evaluated by haematoxylin and eosin.

2.5 | Immunofluorescence and immunohistochemistry staining

Immunofluorescence staining (IF) and immunohistochemistry (IHC) staining was performed on paraffin sections deparaffinized in CitriSolv Hybrid solution (Decon) and gradually rehydrated. Permeabilization was done with 0.1% Tween-20 or 0.05% Triton X-100 in TBS (TBST). For antigen retrieval, the Target Retrieval Solution (Dako) or Tris-EDTA buffer (10 mM Tris base, 1 mM EDTA solution, 0.05% Tween-20, pH 9.0) for KRT10 was used at 95°C for 20–30 min, then cooled at room temperature for 30 min and washed in PBS and PBST. Blocking was done with 10% normal serum in PBS at room temperature for 1.5 h. The sections were incubated overnight at 4°C with the primary antibodies: anti-SFRP2 (1:500, C2C3, Genetex) anti-CD207 (1:100, Novus), anti-beta-catenin (1:500, Thermo Fisher), anti-KRT10 (1:100, RKSE60, Thermo Fisher) or 1 hour at room temperature with anti-KRT5 (1:50, RCK102, Thermo Fisher). For IF of CD207, the biotin-SP AffiniPure donkey anti-rat IgG antibody (1:500, Jackson ImmunoResearch) and Vectastain Elite ABC kit (Vector Labs) were used according to manufacturer recommendations. Following secondary antibodies were used: goat anti-mouse IgG Alexa Fluor Plus 488 (1:500, Thermo Fisher), donkey anti-rabbit Alexa Fluor Plus 488 (1:500, Thermo Fisher), Cy-3-conjugated Streptavidin (1:1000), goat anti-rabbit IgG HRP (1:500, Invitrogen) for 1 hour at room temperature. Nuclei were counterstained using DAPI in SlowFade Gold antifade reagent (Invitrogen). To reduce auto-fluorescence Autofluorescence Reducing Reagent was used (MaxVision). The IF/IHC staining of SFRP2, SFRP2/CD207 and Ki-67 was performed by Histology Core at Northwestern University. Staining without the primary antibodies was performed as a negative control.

2.6 | Fluorescence microscopy

The slides were imaged on a Zeiss LSM880 confocal microscope using 40x or 63x oil objective. The exposure time was identical between controls and experimental slides. The Blue Zen software was used to measure fluorescence intensity.

2.7 | Beta-catenin fluorescence signal quantification

The accumulation and distribution of beta-catenin in individual cells were calculated based on Alexa 488 fluorescence intensity using Blue Zen software (Zeiss). The numerical values were extracted from

each histogram attached to the collected image. The optical sections were selected based on similar intensity of DAPI, and the mean value of signal intensity (sum of pixels intensity) was calculated from at least four sections, from each Z-stack. Minimum six sections were tested for each tissue sample.

2.8 | HaCaT in vitro culture

The cells were purchased from AddexBio and cultured in 5% CO₂ at 37°C in DMEM GlutaMax medium, supplemented with 10% FBS (Gibco), sodium pyruvate and high glucose. Cells were synchronized in cell cycle by serum starvation for 16 hours, grown to 60% or 100% confluency, and then treated with recombinant protein hrSFRP2 (R&D system) at concentration 20 nM or 40 nM for 6 h. Untreated cells were used as control. Each experiment was performed in triplicates, and collected cells were used for qRT-PCR analysis and cell cycle assay.

2.9 | Cell cycle analysis

Cell cycle analysis was performed using Propidium Iodide Flow Cytometry Kit (Abcam) according to manufacturer's protocol. Briefly, 5x10⁵ cells in single cell suspension were fixed in 66% ethanol, then rehydrated in PBS and stained with Propidium iodide for 30 min at 37°C in the dark with presence of RNaseA. The signal intensity was measured on flow cytometer (BD FACS Aria SORP 5-Laser, Biosciences) at 488 nm laser illumination and analysed at Northwestern University Flow Cytometry Core Facility.

2.10 | Quantitative analysis of Langerhans cells number

At least 10 microscopic fields per each section ($n \geq 3$) were photographed and analysed; the number of LCs was assessed based on expression of CD207 (Novus).

2.11 | Normal human skin sections

The normal human skin tissue was purchased from the Northwestern University Mouse Histology and Phenotyping Laboratory.

2.12 | Statistics

All statistics were performed using GraphPad Prism 7 software (GraphPad Software, Inc.). The significance of obtained results was calculated with unpaired Student t-test. All experimental results are presented as mean \pm SD. p values ≤ 0.05 were considered as significant.

3 | RESULTS

3.1 | Transcriptional activation of *SFRP2* correlates with a magnitude of expansion

Our most recent RNA-seq analysis revealed *SFRP2* among the top of the differentially expressed genes in TE. Therefore, we evaluated *SFRP2* transcription levels in skin samples collected at eight timepoints of expansion, from three locations on the expanded skin, by qRT-PCR. Subcutaneously placed expanders were filled with saline to induce acute stretch for one hour (Ex-1h), 24 h (Ex-24h), 3 days (Ex-3d) and 7 days (Ex-7d). A second experimental group received two injections of saline over either 10 days or 14 days (Figure S1a,b). The full-thickness skin biopsies were harvested from the apex ('a'), middle ('b') and peripheral ('d') sites of the expanded skin (Figure S1c). Similar locations on the contralateral side served as controls ('C'). Comprehensive examination of *SFRP2* transcription in all collected biopsies confirmed a correlation between the biopsy position/magnitude of stretch and transcriptional upregulation (Figure 1A). The highest increase in *SFRP2* transcription was detected at the apex of the expanded skin ('a'), where the highest stretching force was applied. The fold change in the 'a' biopsies over the control level was as follows:

37 ± 17 ($p = 0.0057$), 59 ± 16 ($p < 0.0001$), 28 ± 7 ($p = 0.001$) and 16 ± 3 ($p < 0.0001$) for Ex-1h, Ex-24h, Ex-3d and Ex-7d model, respectively. Type 'd' biopsies, collected from the periphery of the expanded skin, revealed no statistically significant changes (Figure 1A). Henceforth, apex samples were examined in this study unless specified otherwise.

To parallel clinical practice, in which subcutaneous expanders are refilled weekly to sustain stretching, we continued TE in four models for a total expansion time of 10 or 14 days. These expanders were filled twice, 7 days apart, two models with 30 ml and two with 60 ml each time. Again, the highest *SFRP2* activation was observed in the 'a' biopsies, $FC = 74 \pm 15$ ($p = 0.0003$) for Ex-10d⁽⁷⁺³⁾*, corresponding to injections of 30 ml at 10 days and 3 days before the tissue was harvested (Figure 1A). Much smaller upregulation, $FC = 2.5 \pm 0.1$ ($p = 0.0005$), for Ex-10d⁽⁷⁺³⁾ was observed when the expander was filled twice with 60 ml. Similar results were obtained for double-filled 14-day TE models: transcription increased by $FC = 12 \pm 8$ ($p = 0.0149$) in Ex-14d⁽⁷⁺⁷⁾* (twice 30 ml) and by 5 ± 3 ($p = 0.0469$) in Ex-14d⁽⁷⁺⁷⁾ (twice 60 ml). These results suggest that in prolonged and repeated stretching, smaller volume/lower stress favours higher transcriptional activation of *SFRP2*.

Next, we compared *SFRP2* expression with the expression pattern of known mechanosensitive genes such as *TNC* (Tenascin-C),

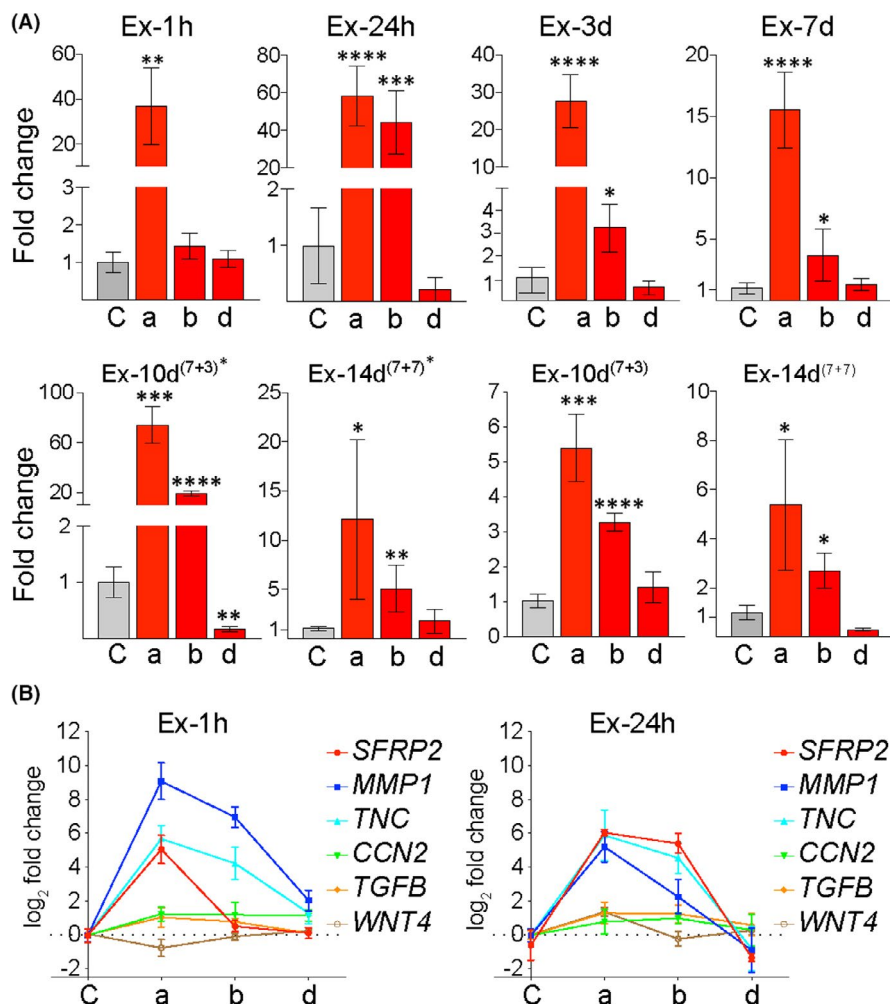


FIGURE 1 Mechanically induced *SFRP2* expression correlates with a magnitude of stretch and presents similar pattern to known genes involved in mechanotransduction. (A) Quantitative analysis of *SFRP2* expression mapped from one hour to 14 days of TE in skin biopsies harvested from the apex ('a'), the middle ('b') and the periphery ('d') of expanded skin. The relative expression was assessed by qRT-PCR and compared to contralateral unexpanded controls. The values were normalized to *B2M* expression and are presented as the averages for at least three biopsies. Error bars represent SD. Statistical significance are shown as * $p \leq 0.05$, ** $p \leq 0.01$, *** $p \leq 0.001$, **** $p \leq 0.0001$. (B) Gene expression pattern of *SFRP2* and known mechanosensitive genes after one hour (Ex-1h) and 24 h (Ex-24h) of expansion

CCN2 (Connective Tissue Growth Factor 2), MMP1 (Matrix Metalloproteinase 1), TGF β 1 (Transforming Growth Factor Beta 1) and WNT4 (Wnt Family Member 4).²⁴⁻²⁸ As presented in Figure 1B, among genes included in this analysis, SFRP2 was one of the three most activated genes in the apical biopsies ('a') in both Ex-1h and Ex-24h models, and its expression presented a similar pattern to other tested genes. This similarity suggests that SFRP2 may also be a mechanosensitive gene.

3.2 | Langerhans cells are a source of SFRP2 in the epidermis

To explore the role of SFRP2 in TE, we first examined the localization of SFRP2⁺ cells by immunohistochemistry staining (IHC), which revealed evenly distributed SFRP2⁺ cells, morphologically similar to dendritic cells, along the epidermis (Figure 2A). SFRP2⁺, likely dendritic, cells were further examined using double immunofluorescence staining (IF) with an antibody against CD207 (Langerin)²¹ (Figure 2B). The co-localization of these proteins identified LCs (CD207⁺) as the main source of SFRP2. SFRP2 and CD207 proteins were visible along the LCs dendrites in both control and expanded skin sections, which indicates that SFRP2 is also expressed by LCs in steady-state conditions. A small number of melanocytes were also positive for SFRP2, as identified by the residual presence of melanin on tissue sections. In addition, we noticed the presence of SFRP2 in dermal fibroblasts, as previously described.²⁹

To examine if LCs secrete SFRP2 in human epidermis, we performed analogous double IF staining on normal human skin samples (Figure S1d). Similar to porcine skin, we observed expression and co-localization of CD207 and SFRP2 on human skin samples in dendritic-like cells. This result shows molecular similarity between porcine and human skin and indicates potential to apply the findings presented in this report to clinical settings.

3.3 | Tissue expansion stimulates Langerhans cell proliferation and migration

To better characterize CD207⁺SFRP2⁺ cells, we calculated their quantity and location under normal and experimental conditions. We found that the number of CD207⁺SFRP2⁺ cells, calculated per image, was two times higher at 1 hour (Ex-1h, $p < 0.0001$), 24 h (Ex-24h, $p = 0.0008$) and 7 days of TE (Ex-7d, $p = 0.0003$) (Figure 2C). The increase in the number of CD207⁺SFRP2⁺ cells was also observed after counts were normalized to the basement membrane length, indicating that TE induces secretion of SFRP2 by LCs (Figure 2C).

CD207⁺SFRP2⁺ cells also gradually migrated upward during TE, reaching statistically significant difference in the number of cells located in basal and suprabasal layers by the 7th day (Figure 2D). To further examine the network of LCs in the epidermis, we calculated

CD207⁺ cell density and compared it with epidermal thickness, defined as surface area of the epidermis on histological cross-sections. This showed that at the 7th day of TE, the thickness of the epidermis increased by $68\% \pm 9\%$ ($p < 0.0001$), and LC density was reduced by $32\% \pm 14\%$ ($p = 0.0041$), suggesting that the network of LCs was not fully rebuilt by the end of the first week of stretching (Figure 2E).

Given that more CD207⁺SFRP2⁺ cells were detected in expanded skin, we performed double IF staining for CD207 and Ki-67 to assess if mechanical forces stimulate LC proliferation. Quantitative analysis revealed that the number of CD207⁺Ki-67⁺ positive cells increased twofold at Ex-1h (FC = 2.4 ± 0.3 , $p < 0.0001$) and Ex-24h (FC = 1.9 ± 0.3 , $p = 0.0011$), and normalized at the 7th day of TE (Figure 2F,G). The increased proliferation of LCs and the migratory shift upward indicates that LCs reorganize themselves, presumably restoring a steady network within the rapidly growing epidermis stimulated by TE.

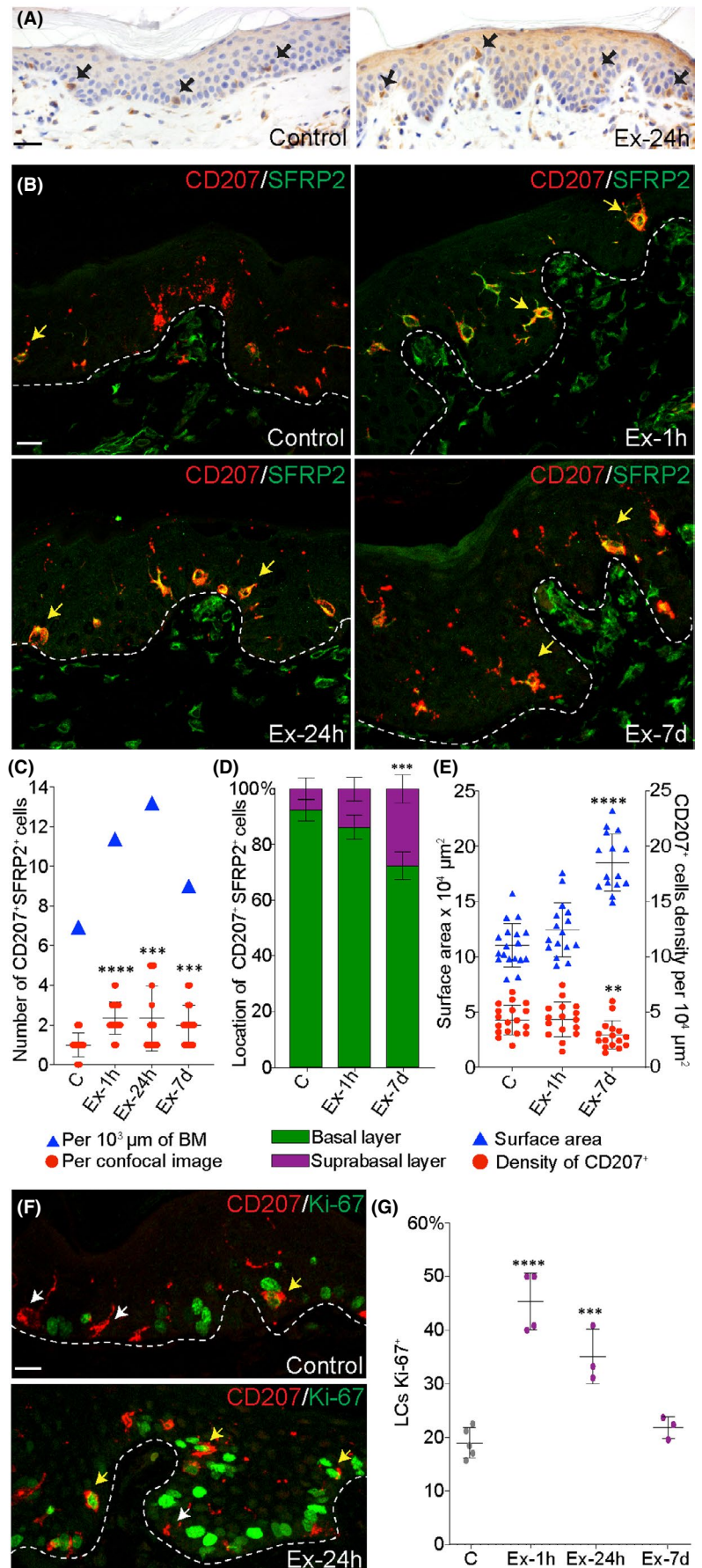
3.4 | SFRP2 augments the maturation of keratinocytes

To further investigate the effect of SFRP2 on KCs, we used a confluent culture of human KCs (HaCaT cells) as an *in vitro* model of normal unperturbed epidermis.³⁰ The SFRP2 recombinant protein (rhSFRP2) was delivered for 6 hours in two different concentrations, either 20 nM or 40 nM, to HaCaT cell culture. Testing for cell cycle progression, we found a slightly extended G2 phase by $17\% \pm 0.5\%$ ($p = 0.0481$) and by $20\% \pm 1\%$ ($p = 0.0388$), for each respective hrSFRP2 concentration as compared to control, consistent with cell growth and differentiation (Figure 3A).

The transition of basal precursors into the suprabasal layer is associated with a transcriptional switch from KRT5 to KRT10,³¹ resulting in cell cycle withdraw and commitment to terminal differentiation. The examination of KRT10 and KRT5 transcription showed an increase in KRT10 expression by 2.7 ± 0.4 times ($p = 0.0035$) and 2.8 ± 0.3 times ($p = 0.0011$) after treatment with 20 nM and 40 nM of rhSFRP2, respectively, and no significant changes in KRT5 expression, indicating augmented cell maturation (Figure 3B). However, hrSFRP2 treatment of the subconfluent culture, representing proliferating KCs in otherwise similar conditions, had no significant effect on cell cycle progression and the expression of KRT5 or KRT10 (Figure S2a,b). Altogether, this suggests that although SFRP2 can stimulate differentiation, it is not the sole stimulator of KC proliferation.

Next, we examined the distribution of KRT10 and KRT5 *in vivo*, using IF on paraffin sections (Figure 3C,D). KRT10 showed regional increases in the suprabasal layer at 24 hours of TE, but the presence of KRT5 was not different among controls and TE samples. These results suggest that mechanical stimulation increased the commitment of basal precursors towards terminal differentiation. Therefore, it seems probable that TE-stimulated expression of SFRP2 augments the early steps of KC maturation *in vivo*.

FIGURE 2 During tissue expansion activated Langerhans cells secrete SFRP2 to epidermal layers of skin through elaborated network of dendrites. Representative images of (A) immunohistochemistry staining of SFRP2 (brown stain) and (B) double immunofluorescent staining of CD207 and SFRP2 in control and expanded skin samples harvested at one hour (Ex-1h), 24 h (Ex-24h) and 7 days (Ex-7d) of expansion. Black arrows in (A) and yellow arrows in (B) indicate SFRP2⁺ and CD207⁺SFRP2⁺ cells, respectively. In (A) slides were counterstained with haematoxylin to mark nuclei (blue stain). (C) Quantitative analysis of double immunofluorescent staining of CD207 and SFRP2. The values are presented as an average number of CD207⁺SFRP2⁺ cells per image (red dots) and per length of basement membrane (BM; blue triangle). (D) Analysis of CD207⁺SFRP2⁺ cells location in the epidermis ($n \geq 10$ images per group) in control and expanded skin harvested at one hour (Ex-1h) and 7 days (Ex-7d) of expansion. (E) Correlation between surface area of the epidermis and density of LCs during tissue expansion at one hour (Ex-1h) and 7 days (Ex-7d) of expansion ($n \geq 10$ images per group). (F) Representative images and (G) quantitative analysis of CD207 and Ki-67 immunofluorescent staining in control and expanded skin samples harvested at one hour (Ex-1h), 24 h (Ex-24h) and 7 days (Ex-7d) of expansion. The yellow and white arrows indicate LCs positive for Ki-67 and negative for Ki-67, respectively. The values are presented as an average number of CD207⁺Ki-67⁺ cells per section ($n \geq 3$ per group). Dashed white dashed lines represent epidermal-dermal junction. Magnification 40 \times , scale bars indicate 10 μ m. Error bars represent SD in (C), (E), (G) and SEM in (D). Significant differences are shown as ** $p \leq 0.01$, *** $p \leq 0.001$, **** $p \leq 0.0001$



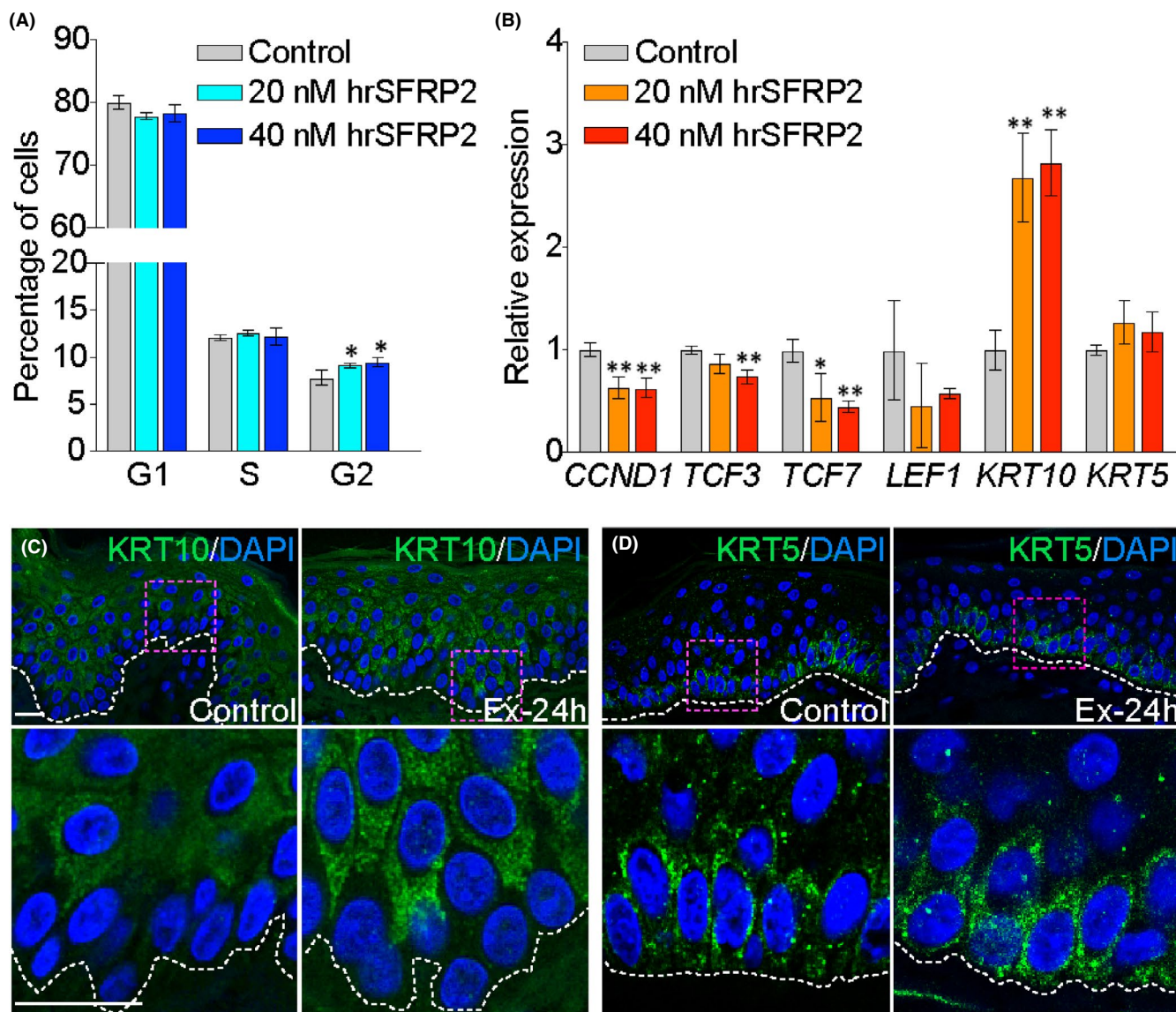


FIGURE 3 Tissue expansion stimulates keratinocytes maturation through increased expression of SFRP2. (A) The cell cycle distribution analysis on human keratinocytes (HaCaT cells) treated with hrSFRP2 ($n = 3$). (B) The expression analysis of Wnt target genes and keratins (*KRT5* and *KRT10*) after in vitro treatment with hrSFRP2 on HaCaT cells ($n = 3$). In (B) the values were normalized to the geometric mean calculated for three references genes: *GAPDH*, *HMBS*, *HPRT1*. Significant differences are shown as * $p \leq 0.05$, ** $p \leq 0.01$, *** $p \leq 0.001$, **** $p \leq 0.0001$. Error bars represent SD. (C, D) Representative images of immunofluorescent staining of (C) KRT10 and (d) KRT5. Bottom panel, which presents the magnified views of the area marked in the top panel, shows regional increase in KRT10 expression but no significant change in KRT5 expression in the expanded skin. The white dashed lines represent epidermal-dermal junction. Magnification 40 \times , scale bar indicates 10 μm

3.5 | SFRP2 inhibits Wnt signalling in in vitro culture of keratinocytes

Since SFRP2 is well recognized as a modifier of Wnt signalling, we evaluated the transcription of Wnt target and effector genes, including *CCND1* (*Cyclin D1*), *TCF3* (Transcription Factor 3), *TCF7* (Transcription Factor 7) and *LEF1* (Lymphoid Enhancer Binding Factor 1), using the cell culture conditions described above. The transcription of tested genes was reduced in a dose-dependent manner (Figure 3B). Specifically, *CCND1* was reduced by $36\% \pm 6\%$ ($p = 0.007$) and $37\% \pm 2\%$ ($p = 0.0051$), *TCF3* by $13\% \pm 1\%$ ($p = 0.0814$)

and $26\% \pm 2\%$ ($p = 0.0042$), *TCF7* by $46\% \pm 17\%$ ($p = 0.0387$) and $56\% \pm 8\%$ ($p = 0.0016$) for 20 nM and 40 nM, respectively, without significant change in *LEF1* transcription. These data indicate the inhibitory effect of rhSFRP2 on Wnt signalling.

3.6 | Tissue expansion affects the subcellular distribution of beta-catenin

Cells' ability to respond to mechanical forces by activating specific signalling pathways allows them to adapt to changing

environments. To investigate the effect of TE on Wnt/beta-catenin signalling activation in KCs and LCs, we evaluated cellular localization of beta-catenin in skin biopsies after one hour (Ex-1h) and 24 h (Ex-24h) of expansion (Figure 4A-F). We observed similar increase by 42%–45% ($p \leq 0.0002$) in nuclear beta-catenin localization in basal KCs ($42\% \pm 12\%$, $p = 0.0001$) and in KCs adjacent to LCs ($CD207^+$ cells; $45 \pm 24\%$, $p = 0.0002$) after one hour of expansion (Ex-1h) (Figure 4A-B',D,E). Interestingly, the nuclear accumulation of

beta-catenin in these cells declined to control level by 24 h of expansion (Figure 4A-E). These results reveal that b-catenin translocation to the nuclei of KCs is stimulated directly by stretch and not by the proximity of LCs. Accordingly, we predict that the force inflicted by TE initiates signalling of beta-catenin, which translocates to the nuclei of KCs and induces KC proliferation.

By contrast, beta-catenin measured in the nuclei of LCs was unchanged at one hour, but increased by $49\% \pm 23\%$ ($p = 0.0094$) at

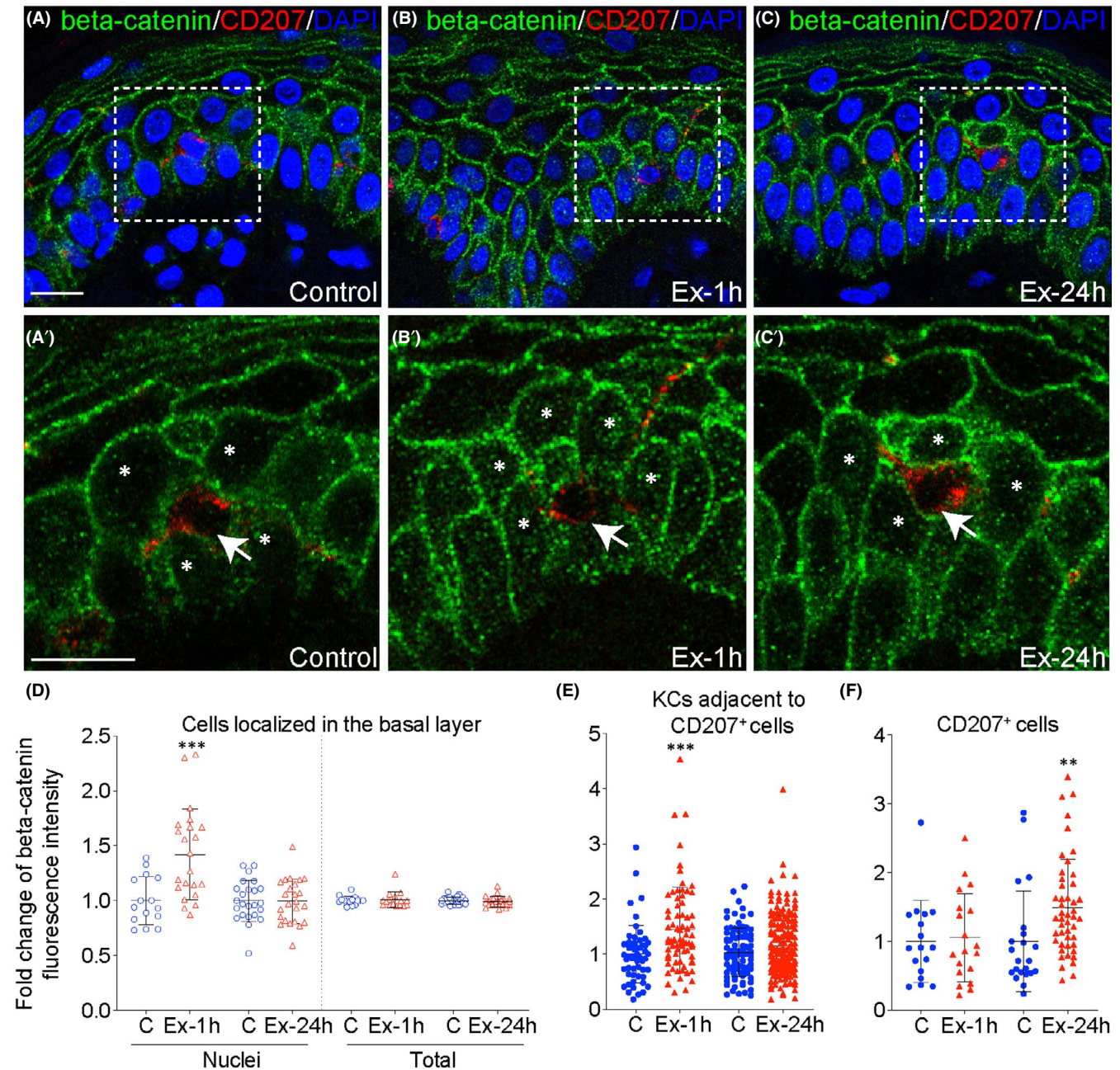


FIGURE 4 Tissue expansion induces beta-catenin translocation to nuclei of basal keratinocytes and Langerhans cells. (A–C') Double immunofluorescent staining of beta-catenin and CD207 counterstained with DAPI to mark nuclei. In panel (A'–C') are the magnified views of the area marked by white squares in (A–C). The arrows and asterisks indicate CD207⁺ cells and keratinocytes adjacent to CD207⁺, respectively. Magnification 40 \times , scale bar indicates 10 μ m. (D–F) Quantitative analysis of beta-catenin intensity in nuclei of (D) basal keratinocytes ($n \geq 15$ images), (E) keratinocytes adjacent to CD207⁺ cells ($n \geq 60$ cells), and (F) CD207⁺ cells ($n \geq 17$ cells). Each dot represents average value for image in (D) and single cells in (E, F). Values represent fold changes between controls and tested samples, and the average value for control was set as one. Significant differences are shown as ** $p \leq 0.01$, *** $p \leq 0.001$. Error bars represent SD

24 h of TE (Figure 4F). The total amount of beta-catenin in basal KCs and LCs was not changed, confirming that the protein had been translocated. These results show that TE induces activation of Wnt/beta-catenin pathway exclusively in basal KCs and LCs. The temporal shift in nuclear accumulation of beta-catenin in the nuclei of these cells reflects a difference in their mechanosensitivity.

4 | DISCUSSION

Our study aimed to better understand the molecular effects of mechanical stretching on the multilayered epidermis. Structurally and functionally, porcine skin is considered very similar to human's and more suitable for experimental models of TE than 'loose-skinned' rodents.³² Porcine and human epidermis, unlike mouse, possess rete ridges which are highly impacted by expansion.⁷

We found that mechanical stretching, inflicted by TE, upregulates *SFRP2* expression, and its transcription level strongly correlates with the magnitude of stretch, corresponding to the location of biopsies. We discovered that LCs proliferate and migrate in response to stretch, and secrete SFRP2 by elongated dendrites to different layers throughout the epidermis. We also assert that SFRP2 may be a mechanosensitive gene as its expression pattern in TE is similar to genes known to respond to mechanical forces. Our studies suggest that SFRP2 augments KC maturation rather than proliferation, which is controlled instead by Wnt/beta-catenin.

The observed upregulation of *SFRP2* expression in expanded skin is likely caused directly by mechanical stretch. The literature supports this assertion by showing that mechanical forces can directly stretch chromatin and induce gene transcription.³³ However, a positive correlation between the relatively highest *SFRP2* transcription level (Figure 1A) and nuclear accumulation of beta-catenin in LCs (Figure 4F) also suggests that *SFRP2* may act downstream of Wnt signalling. There are similarities in the response to strain between bone and skin cells, which support this assumption. For example, mechanical force is known to increase the expression of Wnt/beta-catenin target genes, including *Sfrp1* and *Cnd1*, in osteoblasts and osteoclasts.³⁴⁻³⁶ *Sfrp2* was also identified as the most upregulated extracellular antagonist of Wnt signalling in a Splotch-delayed mouse embryo model of bone and joint development.²⁸ Additionally, in our study, the activation of *SFRP2* in expanded skin closely resembles the transcriptional dynamics of known mechanosensitive genes such as *TNC* and *MMP1*.²⁴⁻²⁸ In conclusion, the transcription of *SFRP2*, activated either by chromatin stretching or Wnt/b-catenin, is induced by mechanical stimuli with a similar pattern to mechanosensitive genes. Furthermore, as expansion is prolonged, SFRP2 expression declines as skin adapts to stretch by growing, attempting to restore homeostasis.

Moreover, we discovered that LCs are the main source of SFRP2 in the epidermis and that stretch stimulates their proliferation and migration from the basal to suprabasal layer, presumably to restore the homeostatic network. This resembles LC behaviour during

wound healing.³⁷ LCs are a unique cell type; based on their ontology, they belong to tissue-resident macrophages, but they function as dendritic cells programmed by interactions with the microenvironment. Signals, such as cytokines, chemokines, pathogens and UV radiation, can induce transcriptional changes in LCs,³⁸ and their proliferation.^{19,39} The decrease in LCs density in the epidermis at 7 days of expansion suggests that mechanically stimulated excessive epidermal growth, driven mostly by KC proliferation, results in temporal disruption in LCs network and homeostasis. Consequently, observed in this study, increased proliferation and migration of LCs, and SFRP2 secretion are driven by mechanical forces likely in an attempt to adapt to homeostatic disruption caused by skin expansion.

We observed that after one our of expansion, Wnt signalling is exclusively activated in basal KCs, preceding the stretched-induced peak in KC proliferation.⁸ Our results are in agreement with data showing that quiescent epithelial cells exposed to mechanical strain re-enter the cell cycle through activation of the beta-catenin pathway.⁴⁰ Numerous studies indicate that Wnt/beta-catenin signalling controls proliferation of basal precursors in the epidermis.⁴¹⁻⁴³ Loss of beta-catenin in the interfollicular epidermis (IFE) results in reduced basal cell proliferation and epidermal thinning, and conversely, transient activation of epidermal beta-catenin leads to increased IFE thickness.^{41,44} In the plasma membrane, beta-catenin is bound to E-cadherin and alpha-catenin complex through adherens junctions, which are involved in mechanotransduction.⁴⁵ Importantly, it has been shown that the E-cadherin/beta-catenin complex at the adherence junction can be opened by physiological strain *in vivo*, which allows a fraction of beta-catenin to be released and translocate to the nucleus to activate transcription.⁴⁶ Several other studies identified beta-catenin as an effector of mechanical signals.^{47,48} Our data from *in vivo* and *in vitro* studies suggest that increased *SFRP2* expression in expanded skin might prevent excessive activation of Wnt/beta-catenin pathway in basal KCs. These results are in agreement with other papers reporting SFRP2 as a Wnt pathway antagonist.⁴⁹⁻⁵¹

Interestingly, at 24 h of expansion, Wnt signalling was no longer upregulated in basal KCs, but nuclear beta-catenin was now increased in LCs. LCs are firmly tethered to KCs through E-cadherin, which is complexed with beta-catenin, located at adherens junction,⁵² and this connection is important for LC migration and maturation.⁵³ It was also shown that beta-catenin is a positive regulator of LC differentiation in response to TGF-beta-1⁵⁴ and breaking the E-cadherin bond on dendritic cells leads to the activation of beta-catenin/TCF/LEF dependent transcription.⁵⁵ Therefore, the increase in beta-catenin accumulation in LCs nuclei indicate temporal disruption in the connection between KCs and LCs, and explains the observed increase in LCs migratory activity under mechanical forces.

Based on *in vitro* treatment of KCs with hrSFRP2 showing increased KRT10 expression, a marker of KC differentiation³¹ and cell cycle progression, we predict that a role of SFRP2 in TE is to stimulate KC differentiation. Consistent with the current understanding of Wnt signalling's role in IFE,⁴¹ KCs which encounter more SFRP2, resulting in less Wnt activity, would progress towards differentiation as shown by the increased expression of KRT10 *in vitro* and *in vivo*. A

previous study even showed that SFRP2 can inhibit KC proliferation in longer treatment.⁵⁶

In conclusion, we have outlined a mechanism through which LCs and SFRP2 act as regulators of epidermal homeostasis in TE. Their mechanically stimulated activation prevents overstimulation of the Wnt/beta-catenin signalling pathway. Although TE typically takes several weeks to generate enough skin for surgical reconstruction, this study indicates that stretching skin initiates molecular responses in as little as one hour. A better understanding of the initiating components of skin growth can contribute to creating skin pre-treatments to stimulate faster growth and regeneration, even in compromised tissue. Our investigation of LCs and SFRP2 highlights their therapeutic potential in this effort.

5 | CONCLUSIONS

In conclusion, our study provides previously unreported evidence that mechanical forces can stimulate SFRP2 secretion by LCs to promote skin growth and restore epidermal homeostasis. This effect is achieved by regulation of Wnt/b-catenin signalling, resulting in augmentation of KC maturation. Altogether, our work uncovers a new biological role for SFRP2 and LCs in mechanically induced skin growth and regeneration, and helps us understand the molecular response of skin during TE.

ACKNOWLEDGEMENTS

Histology services were provided by the Northwestern University Mouse Histology and Phenotyping Laboratory which is supported by NCI P30-CA060553 awarded to the Robert H. Lurie Comprehensive Cancer Center, the Northwestern University Pathology Core Facility, Microscopy and Histology Group at Stanley Manne Children's Research Institute affiliated with Ann and Robert H. Lurie Children's Hospital of Chicago. Surgical procedures were performed at Animal core of Center for Comparative Medicine at Northwestern University.

CONFLICT OF INTEREST

The authors have no conflict of interest to declare. This work was prepared while Jacek Topczewski and Jolanta M. Topczewska were employed at Lurie Children's Hospital of Chicago and Northwestern University. The opinions expressed in this article are the author's own and do not reflect the view of the National Institutes of Health, the Department of Health and Human Services, or the United States government.

AUTHOR CONTRIBUTIONS

Joanna K. Ledwon: Conceptualization (equal); Data curation (lead); Formal analysis (lead); Investigation (lead); Methodology (lead); Visualization (lead); Writing – original draft (equal). **Elbert E. Vaca:** Investigation (supporting); Writing – review & editing (supporting). **Chiang C. Huang:** Resources (equal); Writing – review & editing (supporting). **Lauren J Kelsey:** Investigation (supporting); Writing

– review & editing (equal). **Jennifer L. McGrath:** Investigation (supporting); Writing – review & editing (supporting). **Jacek Topczewski:** Resources (equal); Writing – review & editing (supporting). **Arun K. Gosain:** Conceptualization (supporting); Funding acquisition (lead); Supervision (equal); Writing – review & editing (supporting). **Jolanta M. Topczewska:** Conceptualization (equal); Formal analysis (supporting); Funding acquisition (supporting); Investigation (supporting); Methodology (equal); Supervision (lead); Visualization (supporting); Writing – original draft (lead).

DATA AVAILABILITY STATEMENT

All data generated or analysed during this study are included in this article and its supplementary information files.

ORCID

Joanna K. Ledwon  <https://orcid.org/0000-0001-8047-4334>

REFERENCES

- Zollner AM, Holland MA, Honda KS, Gosain AK, Kuhl E. Growth on demand: reviewing the mechanobiology of stretched skin. *J Mech Behav Biomed Mater.* 2013;28:495-509.
- Purnell CA, Gart MS, Buganza-Tepole A, et al. Determining the differential effects of stretch and growth in tissue-expanded skin: combining isogeometric analysis and continuum mechanics in a porcine model. *Dermatol Surg.* 2018;44(1):48-52.
- Summerfield A, Meurens F, Ricklin ME. The immunology of the porcine skin and its value as a model for human skin. *Mol Immunol.* 2015;66(1):14-21.
- Ledwon JK, Kelsey LJ, Vaca EE, Gosain AK. Transcriptomic analysis reveals dynamic molecular changes in skin induced by mechanical forces secondary to tissue expansion. *Sci Rep.* 2020;10(1):15991.
- Lee T, Vaca EE, Ledwon JK, et al. Improving tissue expansion protocols through computational modeling. *J Mech Behav Biomed Mater.* 2018;82:224-234.
- Turin SY, Ledwon JK, Bae H, Buganza-Tepole A, Topczewska J, Gosain AK. Digital analysis yields more reliable and accurate measures of dermal and epidermal thickness in histologically processed specimens compared to traditional methods. *Exp Dermatol.* 2018;27(6):687-690.
- Topczewska JM, Ledwon JK, Vaca EE, Gosain AK. Mechanical stretching stimulates growth of the basal layer and rete ridges in the epidermis. *J Tissue Eng Regen Med.* 2019;13(11):2121-2125.
- Janes LE, Ledwon JK, Vaca EE, et al. Modeling tissue expansion with isogeometric analysis: skin growth and tissue level changes in the porcine model. *Plast Reconstr Surg.* 2020;146(4):792-798.
- Kawano Y, Kypta R. Secreted antagonists of the Wnt signalling pathway. *J Cell Sci.* 2003;116(Pt 13):2627-2634.
- Esteve P, Sandonis A, Ibanez C, Shimono A, Guerrero I, Bovolenta P. Secreted frizzled-related proteins are required for Wnt/beta-catenin signalling activation in the vertebrate optic cup. *Development.* 2011;138(19):4179-4184.
- Lin H, Angeli M, Chung KJ, Ejimadu C, Rosa AR, Lee T. sFRP2 activates Wnt/ β -catenin signaling in cardiac fibroblasts: differential roles in cell growth, energy metabolism, and extracellular matrix remodeling. *Am J Physiol Cell Physiol.* 2016;311(5):C710-C719.
- Alfaro MP, Pagni M, Vincent A, et al. The Wnt modulator sFRP2 enhances mesenchymal stem cell engraftment, granulation tissue formation and myocardial repair. *Proc Natl Acad Sci U S A.* 2008;105(47):18366-18371.
- Mirotosu M, Zhang Z, Deb A, et al. Secreted frizzled related protein 2 (Sfrp2) is the key Akt-mesenchymal stem cell-released paracrine

- factor mediating myocardial survival and repair. *Proc Natl Acad Sci U S A*. 2007;104(5):1643-1648.
14. Kim M, Han JH, Kim JH, Park TJ, Kang HY. Secreted frizzled-related protein 2 (sFRP2) functions as a melanogenic stimulator; the role of sFRP2 in UV-induced hyperpigmentary disorders. *J Invest Dermatol*. 2016;136(1):236-244.
 15. Sun Y, Zhu D, Chen F, et al. SFRP2 augments WNT16B signaling to promote therapeutic resistance in the damaged tumor microenvironment. *Oncogene*. 2016;35(33):4321-4334.
 16. Kaplan DH. Ontogeny and function of murine epidermal Langerhans cells. *Nat Immunol*. 2017;18(10):1068-1075.
 17. Deckers J, Hammad H, Hoste E. Langerhans cells: sensing the environment in health and disease. *Front Immunol*. 2018;9:93.
 18. Stojadinovic O, Yin N, Lehmann J, Pastar I, Kirsner RS, Tomic-Canic M. Increased number of Langerhans cells in the epidermis of diabetic foot ulcers correlates with healing outcome. *Immunol Res*. 2013;57(1-3):222-228.
 19. Chorro L, Sarde A, Li M, et al. Langerhans cell (LC) proliferation mediates neonatal development, homeostasis, and inflammation-associated expansion of the epidermal LC network. *J Exp Med*. 2009;206(13):3089-3100.
 20. Nfon CK, Dawson H, Toka FN, Golde WT. Langerhans cells in porcine skin. *Vet Immunol Immunopathol*. 2008;126(3-4):236-247.
 21. Valladeau J, Ravel O, Dezutter-Dambuyant C, et al. Langerin, a novel C-type lectin specific to Langerhans cells, is an endocytic receptor that induces the formation of Birbeck granules. *Immunity*. 2000;12(1):71-81.
 22. Nair X, Tramosch KM. The Yucatan miniature swine as an in vivo model for screening skin depigmentation. *J Dermatol Sci*. 1991;2(6):428-433.
 23. Livak KJ, Schmittgen TD. Analysis of relative gene expression data using real-time quantitative PCR and the 2(-Delta Delta C(T)) Method. *Methods*. 2001;25(4):402-408.
 24. Imanaka-Yoshida K, Matsumoto KI. Multiple roles of tenascins in homeostasis and pathophysiology of aorta. *Ann Vasc Dis*. 2018;11(2):169-180.
 25. Blaauw E, Lorenzen-Schmidt I, Babiker FA, et al. Stretch-induced upregulation of connective tissue growth factor in rabbit cardiomyocytes. *J Cardiovasc Transl Res*. 2013;6(5):861-869.
 26. Goto T, Mikami KI, Miura K, et al. Mechanical stretch induces matrix metalloproteinase 1 production in human hepatic stellate cells. *Pathophysiology*. 2004;11(3):153-158.
 27. Sakata R, Ueno T, Nakamura T, Ueno H, Sata M. Mechanical stretch induces TGF-beta synthesis in hepatic stellate cells. *Eur J Clin Invest*. 2004;34(2):129-136.
 28. Rolfe RA, Nowlan NC, Kenny EM, et al. Identification of mechanosensitive genes during skeletal development: alteration of genes associated with cytoskeletal rearrangement and cell signalling pathways. *BMC Genom*. 2014;15:48.
 29. Tabib T, Morse C, Wang T, Chen W, Lafyatis R. SFRP2/DPP4 and FMO1/LSP1 define major fibroblast populations in human skin. *J Invest Dermatol*. 2018;138(4):802-810.
 30. Poumay Y, Pittelkow MR. Cell density and culture factors regulate keratinocyte commitment to differentiation and expression of suprabasal K1/K10 keratins. *J Invest Dermatol*. 1995;104(2):271-276.
 31. Fuchs E. Epidermal differentiation: the bare essentials. *J Cell Biol*. 1990;111(6 Pt 2):2807-2814.
 32. Debeer S, Le Ludec JB, Kaiserlian D, et al. Comparative histology and immunohistochemistry of porcine versus human skin. *Eur J Dermatol*. 2013;23(4):456-466.
 33. Tajik A, Zhang Y, Wei F, et al. Transcription upregulation via force-induced direct stretching of chromatin. *Nat Mater*. 2016;15(12):1287-1296.
 34. Case N, Ma M, Sen B, Xie Z, Gross TS, Rubin J. Beta-catenin levels influence rapid mechanical responses in osteoblasts. *J Biol Chem*. 2008;283(43):29196-29205.
 35. Robinson JA, Chatterjee-Kishore M, Yaworsky PJ, et al. Wnt/beta-catenin signaling is a normal physiological response to mechanical loading in bone. *J Biol Chem*. 2006;281(42):31720-31728.
 36. Lau KH, Baylink DJ, Zhou XD, et al. Osteocyte-derived insulin-like growth factor I is essential for determining bone mechanosensitivity. *Am J Physiol Endocrinol Metab*. 2013;305(2):E271-281.
 37. Smith CH, Allen MH, Groves RW, Barker JN. Effect of granulocyte macrophage-colony stimulating factor on Langerhans cells in normal and healthy atopic subjects. *Br J Dermatol*. 1998;139(2):239-246.
 38. Kim JH, Hu Y, Yongqing T, et al. CD1a on Langerhans cells controls inflammatory skin disease. *Nat Immunol*. 2016;17(10):1159-1166.
 39. Li M, Hener P, Zhang Z, Kato S, Metzger D, Chambon P. Topical vitamin D3 and low-calcemic analogs induce thymic stromal lymphopoietin in mouse keratinocytes and trigger an atopic dermatitis. *Proc Natl Acad Sci U S A*. 2006;103(31):11736-11741.
 40. Benham-Pyle BW, Sim JY, Hart KC, Pruitt BL, Nelson WJ. Increasing beta-catenin/Wnt3A activity levels drive mechanical strain-induced cell cycle progression through mitosis. *Elife*. 2016;5:e19799.
 41. Lim X, Tan SH, Koh WL, et al. Interfollicular epidermal stem cells self-renew via autocrine Wnt signaling. *Science*. 2013;342(6163):1226-1230.
 42. Mendoza-Reinoso V, Beverdam A. Epidermal YAP activity drives canonical WNT16/beta-catenin signaling to promote keratinocyte proliferation in vitro and in the murine skin. *Stem Cell Res*. 2018;29:15-23.
 43. Ghahramani A, Donati G, Luscombe NM, Watt FM. Epidermal Wnt signalling regulates transcriptome heterogeneity and proliferative fate in neighbouring cells. *Genome Biol*. 2018;19(1):3.
 44. Choi YS, Zhang Y, Xu M, et al. Distinct functions for Wnt/beta-catenin in hair follicle stem cell proliferation and survival and interfollicular epidermal homeostasis. *Cell Stem Cell*. 2013;13(6):720-733.
 45. Cha B, Geng X, Mahamud MR, et al. Mechanotransduction activates canonical Wnt/beta-catenin signaling to promote lymphatic vascular patterning and the development of lymphatic and lymphovenous valves. *Genes Dev*. 2016;30(12):1454-1469.
 46. Roper JC, Mitrossilis D, Stirnemann G, et al. The major beta-catenin/E-cadherin junctional binding site is a primary molecular mechanotransducer of differentiation in vivo. *Elife*. 2018;7:e33381.
 47. Yonemura S, Wada Y, Watanabe T, Nagafuchi A, Shibata M. alpha-Catenin as a tension transducer that induces adherens junction development. *Nat Cell Biol*. 2010;12(6):533-542.
 48. Wang J, Zhang Y, Zhang N, Wang C, Herrler T, Li Q. An updated review of mechanotransduction in skin disorders: transcriptional regulators, ion channels, and microRNAs. *Cell Mol Life Sci*. 2015;72(11):2091-2106.
 49. Jin L, Cao Y, Yu G, et al. SFRP2 enhances the osteogenic differentiation of apical papilla stem cells by antagonizing the canonical WNT pathway. *Cell Mol Biol Lett*. 2017;22:14.
 50. Zhang Z, Deb A, Zhang Z, et al. Secreted frizzled related protein 2 protects cells from apoptosis by blocking the effect of canonical Wnt3a. *J Mol Cell Cardiol*. 2009;46(3):370-377.
 51. Yang H, Li G, Han N, et al. Secreted frizzled-related protein 2 promotes the osteo/odontogenic differentiation and paracrine potentials of stem cells from apical papilla under inflammation and hypoxia conditions. *Cell Prolif*. 2020;53(1):e12694.
 52. Tang A, Amagai M, Granger LG, Stanley JR, Udey MC. Adhesion of epidermal Langerhans cells to keratinocytes mediated by E-cadherin. *Nature*. 1993;361(6407):82-85.
 53. Gaiser MR, Lammermann T, Feng X, et al. Cancer-associated epithelial cell adhesion molecule (EpCAM; CD326) enables epidermal Langerhans cell motility and migration in vivo. *Proc Natl Acad Sci U S A*. 2012;109(15):E889-897.
 54. Yasmin N, Konradi S, Eisenwort G, et al. beta-Catenin promotes the differentiation of epidermal Langerhans dendritic cells. *J Invest Dermatol*. 2013;133(5):1250-1259.

55. Jiang A, Bloom O, Ono S, et al. Disruption of E-cadherin-mediated adhesion induces a functionally distinct pathway of dendritic cell maturation. *Immunity*. 2007;27(4):610-624.
56. Kim BK, Yoon SK. Expression of sfrp2 is increased in catagen of hair follicles and inhibits keratinocyte proliferation. *Ann Dermatol*. 2014;26(1):79-87.

How to cite this article: Ledwon JK, Vaca EE, Huang CC, et al. Langerhans cells and SFRP2/Wnt/beta-catenin signalling control adaptation of skin epidermis to mechanical stretching. *J Cell Mol Med*. 2022;26:764-775. doi:[10.1111/jcmm.17111](https://doi.org/10.1111/jcmm.17111)

SUPPORTING INFORMATION

Additional supporting information may be found in the online version of the article at the publisher's website.